Determinism and divergence of apoptosis susceptibility in mammalian cells

Patrick D. Bhola and Sanford M. Simon*

Department of Cellular Biophysics, The Rockefeller University, 1230 York Avenue, New York, NY 10065, USA
*Author for correspondence (simon@rockefeller.edu)

Accepted 15 September 2009
Journal of Cell Science 122, 4296-4302 Published by The Company of Biologists 2009
doi:10.1242/jcs.055590

Summary

Although the cellular decision to commit to apoptosis is important for organism homeostasis, there is considerable variability in the onset of apoptosis between cells, even in clonal populations. Using live single-cell imaging, we observed that the onset of apoptotic proteolytic activity was tightly synchronized between nearby cells. This synchrony was not a consequence of secreted factors and was not correlated to the cell cycle. The synchrony was only seen amongst related cells and was lost over successive generations. The times of apoptosis also diverged within a generation, but this was blocked by inhibiting protein synthesis before triggering apoptosis. These results suggest that the cell-cell variability of apoptosis times is due to the divergence of the molecular composition of the cell, and that the decision to commit to apoptosis at the time of drug addition is a deterministic decision.

Supplementary material available online at
http://jcs.biologists.org/cgi/content/full/122/23/4296/DC1

Key words: Fluorescence microscopy, Protease, Caspase, Lineage, Epigenetics

Introduction

Apoptosis is a form of cell death that eliminates unwanted or harmful cells (Ellis et al., 1991). It is characterized by the activation of caspases (Salvesen and Dixit, 1997; Yuan et al., 1993), DNA fragmentation (Liu et al., 1997) and changes in cellular morphology (Wyllie, 1980). In response to apoptotic stimuli, a cell must make a decision either to survive or to commit to apoptosis (Danial and Korsmeyer, 2004).

Cells destined to undergo apoptosis in response to internal stresses and some external stresses release cytochrome c and Smac from mitochondria (Ow et al., 2008), and within minutes activate caspase-3 and caspase-9 (Rehm et al., 2003). In contrast to the tight timing between these events, the duration of events preceding cytochrome c release and caspase activation can vary from 1 hour to over 20 hours within a clonal population of cells (Goldstein et al., 2000). This variation is striking considering that the biochemical events within this delayed and variable stage determine whether the cell will die.

Population variability has also been documented for other phenotypes, including phage lambda infection (Arkin et al., 1998), bacterial chemotaxis (Spudich and Koshland, Jr, 1976), cell differentiation (Abkowitz et al., 1996; Enver et al., 1998) and HIV-1 Tat transactivation (Weinberger et al., 2005). Understanding the sources and dynamics of apoptotic variability can lend insight into the precision with which cells are able to process extracellular signals. A number of different factors could contribute to population variability of apoptosis, including differences in the composition of single cells, the local environment of single cells, or stochasticity in biochemical reactions triggered by apoptotic stimuli.

To gain insight into the sources of cell-cell variability in apoptosis, we assayed the activation of proteases that cleave a DEVD sequence in living cells. Although DEVD is cleaved efficiently by caspase-3, it is also cleaved by other proteases activated during apoptosis, including caspase-7 and cathepsin B (Schotte et al., 1999; Thornberry et al., 1997). Live-cell assays enabled correlation of the location of a cell, its lineage and position in the cell cycle, until the eventual time of apoptosis. Although monitoring the cleavage of DEVD can be achieved with FRET reporters, these reporters require the use of two fluorescent proteins, and therefore use a significant portion of the visible spectrum (Nguyen and Daugherty, 2005; Xu et al., 1998).

Here, we report the development of a genetically encoded single fluorophore reporter for cleavage of the peptide DEVD. We found that when and whether cells entered apoptosis were synchronized between cells in close proximity. Entry into apoptosis did not correlate with the distance between unrelated cells, or with the phase of the cell cycle. Entry into apoptosis was strongly correlated for sister cells, and this correlation diverged over subsequent generations. The divergence of apoptosis times was inhibited by blockade of protein synthesis. These results indicate that there is a persistent cellular state underlying the susceptibility of a single cell to apoptosis.

Results

Design of caspase reporter

We created a reporter of caspase activity based on a change of location. We constructed two classes of reporters (Fig. 1A, supplementary material Fig. S1); these were sensitive to cleavage of peptide sequences that are targets for caspases. Upon caspase cleavage, the first reporter should move from the plasma membrane to the cytoplasm (pmDEVD, Fig. 1B), whereas the second reporter should move from the cytoplasmic surface of the endoplasmic reticulum to the nucleus (erDEVD) (supplementary material Fig. S1).

The pmDEVD reporter consists of an N-terminal plasma membrane (pm) targeting palmitoylation domain from GAP-43 (Skene and Virag, 1989) and a fluorescent protein, which are separated by a linker region containing a caspase-3/7 cleavage site

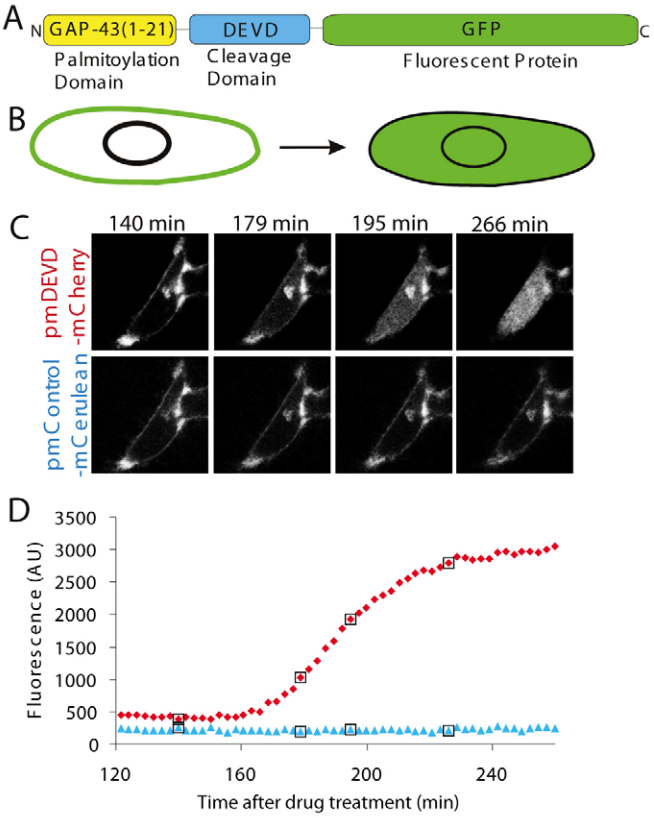

Fig. 1. DEVDase. (A) Cartoon of the design of the pmDEVD reporter. (B) Predicted relocation of the reporter. (C) Time-lapse images of HeLa cells co-expressing the pmDEVD and pmControl reporters after treatment with STS (2 μM). (D) Quantification of the time-lapse image series for pmDEVD. Points with squares correspond to the images displayed in C. Red diamonds, pmDEVD; blue triangles, pmControl.

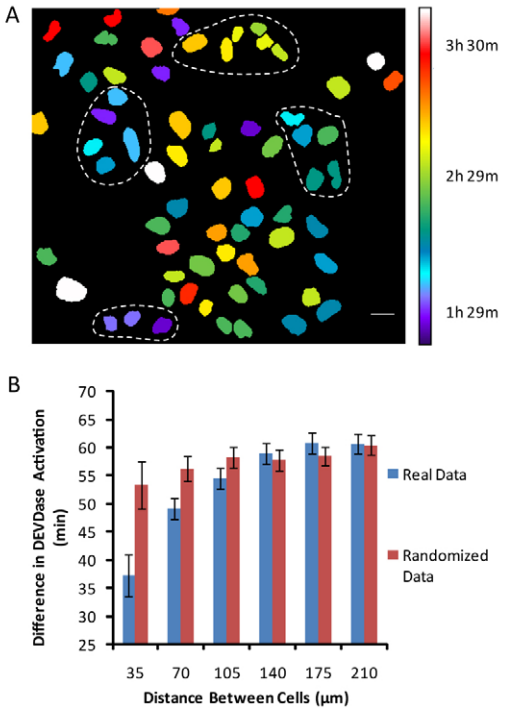

Fig. 2. Local synchronization of apoptosis. (A) Nuclei of HeLa cells treated with 2 μM STS. Nuclei are color coded to represent the times of apoptosis. Clusters of cells with white outlines indicate examples of neighboring cells undergoing DEVDase activation at similar times. (B) Plot of the difference in time of apoptosis between HeLa cells as a function of their distance reveals a correlation between apoptosis and distance. (Error bars represent 95% confidence interval of the mean.)

(Fig. 1A, supplementary material Table S1). The linker region contains the amino acid sequence DEVD that has been used to detect caspase-3/7 activity (Thornberry et al., 1997). However since other proteases can cleave DEVD, we refer to it as a DEVDase reporter. When the mCherry fluorescent protein is used, the resulting probe is referred to as pmDEVD-mCherry. As a control for whether the caspase-sensitive linker region was responsible for any changes in localization, we created a reporter (pmControl) that differed by the absence of the DEVD cleavage site in the linker region (supplementary material Table S1).

Two plasma membrane reporters (pmDEVD-mCherry and pmControl-Cerulean) were co-expressed in HeLa cells. After treatment with staurosporine (STS, 2 μM), mCherry fluorescence relocalized from the plasma membrane to the cytosol (Fig. 1C, supplementary material Movie 1). This was quantified by monitoring the fluorescence in a region within the cytoplasm (Fig. 1D). The pmControl-Cerulean remained at the plasma membrane (Fig. 1C,D), indicating that the DEVD cleavage site is responsible for the change in signal. The lack of change in the pmControl-Cerulean signal also indicates that the contraction of apoptotic cells is not responsible for the increase in the pmDEVD-mCherry signal. Similar results were observed for cells treated with TNFα and cycloheximide (CHX), and with soluble Fas ligand (sFasL) (supplementary material Fig. S2). Changes in the reporter could also be observed with wide-field microscopy (supplementary material Fig. S3A-C).

The relocalization of the reporter could be detected within minutes of the release of cytochrome-c-GFP from mitochondria (supplementary material Fig. S3D,E), and expression of the reporter did not delay TUNEL staining kinetics within a population of cells (supplementary material Fig. S4H). This confirms that these cells are apoptotic and demonstrates that the reporter is not perturbing the biological events. We compared the reporter to existing reporters of caspase activity, and found that the pmDEVD reporter had similar kinetics as a FRET reporter, although with improved signal to noise (supplementary material Fig. S4A-G).

Apoptosis in neighboring cells

To gain insight into cell-to-cell variability in the onset of apoptosis, we monitored apoptosis (STS 2 μM) in HeLa cells expressing pmDEVD-mCherry and a nuclear marker (YFP-NLS) using wide-field microscopy. A map of nuclei that were color coded to represent the time of activation of caspase-3 or caspase-7, suggested that groups of spatially clustered cells underwent apoptosis at similar times and that there is therefore a localized synchronization of apoptosis (Fig. 2A).

To quantify the local synchronization of caspase-3 or caspase-7 activation, we plotted the difference in the time of DEVDase

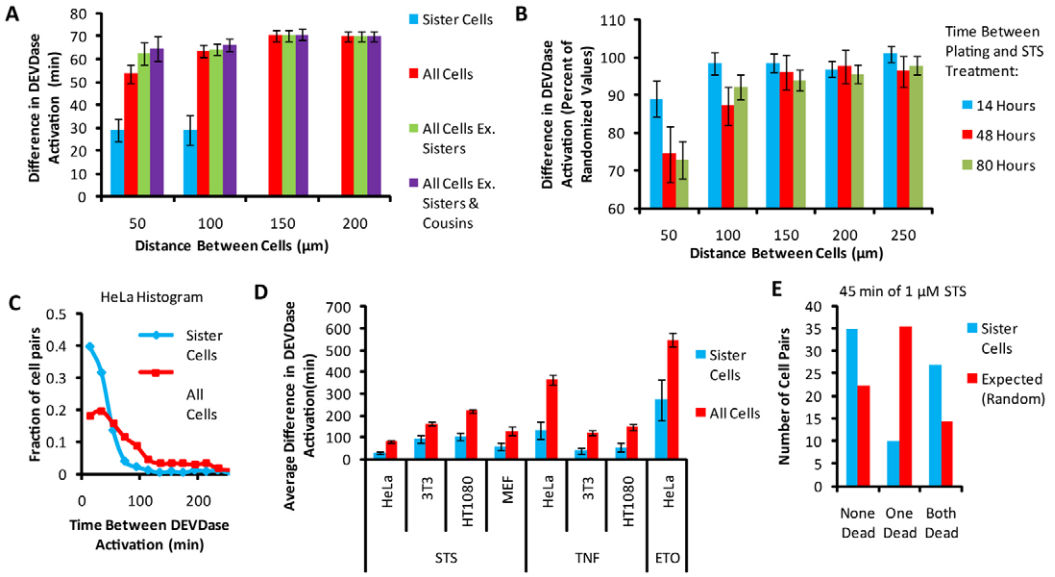

Fig. 3. Distance between cells and initiation of apoptosis. (A) Analysis of the time difference of DEVDase activation as a function of distance between cells for sister cell cells (blue), between all cells (red), between all cells that are not sister cells (green), and between all cells that are not sister cells or cousin cells (purple) (n=562 cells in three fields). (B) Analysis of time difference of DEVDase activation as a function of distance for cells plated at various times prior to STS addition (n_{cells}>385 for each time point). (C) Histogram of the difference in time of DEVDase activation between HeLa sister cells, and between randomly paired cells (n=265 pairs). (D) Average difference in DEVDase activation between sister cells (blue), and randomly paired cells (red) for HeLa, NIH3T3 and HT1080 cells treated with 2 µM STS, 250 ng/µl TNFα + 5 µg/ml CHX, or 50 µM ETO. Differences between sister and random distributions are significant for all cell types (STS: HeLa, P=6.2×10^{-34}; 3T3, P=0.0011; HT1080, P=2.1×10^{-10}; MEF, P=9.9×10^{-4}. TNFα+CHX: HeLa, P=1.4×10^{-16}; 3T3, P=4.7×10^{-14}; HT1080, P=5.8×10^{-10}. ETO: HeLa, P=1.2×10^{-11}. For MEFs, n_{pairs}=21; for all other cells: n_{pairs} is between 54-106 pairs for different conditions). (E) HeLa cells treated with 1 µM STS for 45 minutes. In blue are counts of sister cell pairs where both cells die, only one cell dies and where both survive. In red is the expected value of the counts if there were no apoptosis similarity between sister cells, and given that 44% of all cells underwent apoptosis. All error bars represent the 95% confidence interval of the mean.

activation as a function of the distance between cells. When cells were closer to each other it was more likely that their DEVDase activation would be synchronized (Fig. 2B, blue). To determine potential artifacts of the analysis that could generate a spatial correlation, we randomly reassigned apoptosis times to different cellular positions and no correlation was reported (Fig. 2B, red).

The following are three possibilities that could explain the correlation of the distance between cells and the time of DEVDase activation: (1) cells that are near each other might be sister cells that are at a similar phase of the cell cycle. A cell-cycle-dependent susceptibility to apoptosis could account for the local synchronization of apoptosis. However, neither use of a population synchronized in its cell cycle nor an asynchronous populations with reporters for the cell cycle, revealed a correlation between apoptosis and the cell cycle (supplementary material Figs S5 and S6); (2) Cells might secrete factors that promote or hinder apoptosis in a local neighborhood; (3) sister cells might have similar molecular compositions uncoupled from the cell cycle that affect their sensitivity to entering apoptosis.

Separation of distance and genealogy

To separate the effects of distance and genealogy, we first monitored apoptosis in the rapidly moving HT1080 cell line (supplementary material Fig. S7). In these cell lines, we did not observe a correlation between inter-cell distance and the time of apoptosis (supplementary material Fig. S7). Next, we determined the correlation between DEVDase activation and distance, after excluding comparisons between related HeLa cells (Fig. 3A). Cells at closer distances demonstrated a greater similarity of their times of DEVDase activation than cells further apart, indicating a correlation between DEVDase activation and distance (Fig. 3A, red). However, when sister cells were excluded from the comparison the correlation was weaker (Fig. 3A, green), and weakened further when sister and cousin cells were excluded (Fig. 3A, purple). The reduced spatial correlation when related cells are removed from distance comparisons suggests that a secreted factor does not contribute to the correlation between DEVDase activation and intercellular distance.

The third test was to uncouple distance and genealogy by dissociating cells from their dish, and then re-plating them so their positions are randomized. If the genealogical relationship between cells was responsible for the local synchronization of apoptosis, then when cells were dissociated and then re-plated at a high density, the local effects should be lost. By contrast, effects of secreted factors on neighboring apoptosis should be unaffected. Cells plated 48 hours or 80 hours before STS treatment showed a stronger distance correlation than cells plated 14 hours before STS treatment (Fig. 3B). The combination of the above experiments suggests that secreted factors do not have a role that can be detected in the local synchronization of apoptosis.

Similarity of timing of apoptosis between sister cells

We next directly quantified the distribution of differences in the timing of apoptosis between sister cells (Fig. 3C, blue). As a control, we measured the distribution of the differences in the time of DEVDase activation between randomly paired cells (Fig. 3C, red). The difference in DEVDase activation between randomly paired cells was significantly greater than the difference in DEVDase activation between sister cells (P=6.2×10^{-34}; Fig. 3C).

The average difference in the onset of DEVDase activation between sister cells and between randomly paired cells was

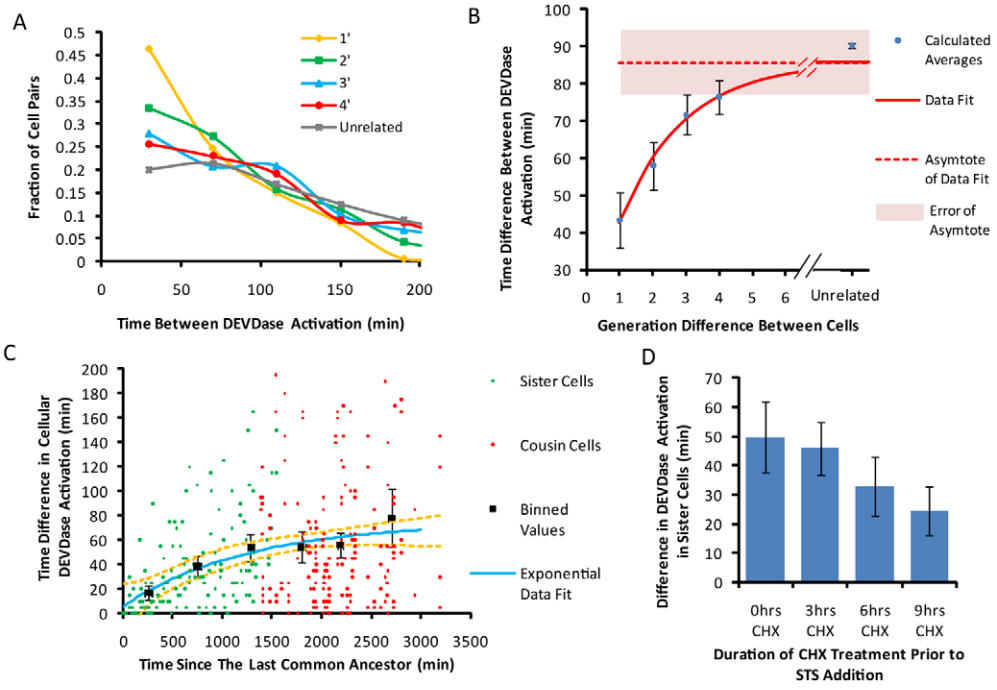

Fig. 4. Divergence of apoptotic susceptibility. (A) The difference in time of apoptosis between cells from different generations. As the number of generations between cells increases, the curve flattens. (B) Analysis of the difference in DEVDase activation between cells from different generations and between unrelated cells (blue circles). Cells are fit to an exponential recovery curve (solid red line). Exponential fit is: y=42.5+43.2(1–e$^{-(g-1)/1.94}$) with y minutes, and g in generational difference between cells; R^2=0.988 for the shown data points. Red dotted line is the asymptote of exponential recovery fit. Pink overlay is the error of the asymptote. (C) Difference in DEVDase activation between related cells (sister cells, green; cousin cells, red) as a function of time since cells shared a common ancestor. Recovering exponential fit (blue line), confidence interval of fit (yellow line) are plotted as well as individual time points from a 500 minute binning (black squares). Exponential fit is: y=5.8+68.5(1–e$^{-t/1256}$) with y and t in minutes; R^2=0.122. (D) Difference in DEVDase activation between newly divided sister cells for different treatments with cycloheximide (see text). Relative to untreated cells, the difference is smaller for cells in CHX for 9 hours (P=0.0039). Error bars represent 95% confidence intervals.

calculated for HeLa, NIH3T3, HT1080 and mouse embryonic fibroblasts (MEF) cells. These cells were treated with STS, TNFα and CHX, or etoposide (ETO) (Fig. 3D). In all cases, the average time difference of DEVDase activation between sister cells was significantly less than the average time difference of DEVDase activation between randomly paired cells. These results indicate that the temporal similarity of apoptosis between sister cells is not a cell-type-specific or drug-specific effect.

Similarity of sister cell fate

To determine whether cell fate was similar between sister cells, we used a milder apoptotic treatment that only killed a fraction of cells, and determined whether both sister cells underwent apoptosis or survived, or whether only one of the sister cells underwent apoptosis. HeLa cells were treated with STS (1 μM) for 45 minutes, and 44% of the cells underwent apoptosis during the subsequent 36 hours. If there was no linkage in the fate between sister cells, then of 72 cell pairs, 14 pairs should both undergo apoptosis, 22 should both survive, and 36 should have only one cell undergoing apoptosis (Fig. 3E, red). Instead, we observed that 27 sister pairs both underwent apoptosis, 35 pairs both survived and there were 10 pairs where only one cell underwent apoptosis (Fig. 3E, blue). Given that 44% of all cells die, the probability that there are only 10 pairs of sister cells of which only one undergoes apoptosis is P<0.0005 (χ^2=37.2, two degrees of freedom). This indicates that not only is the timing of apoptosis between sister cells similar, but also the fates of sister cells are similar when given a mild apoptotic treatment.

Intergenerational divergence of apoptosis susceptibility

We reasoned that if the similarity of apoptosis times between sister cells resulted from a temporary inheritance of proteins, then the difference in the onset of apoptosis between two cells should become larger as the cells are more distantly related. Alternatively, if it were a stable genetic alteration, then the differences in the onset of apoptosis should remain constant for the different lineages.

After monitoring the lineage of HeLa cells for four generations, we treated cells with STS (1 μM) and compared the time of apoptosis between cells that shared a common ancestor. We defined sister cells as being one generation apart, and cousin cells as two generations apart (supplementary material Fig. S8). A graph of the apoptosis time differences, as well as the apoptosis time difference between randomly paired cells is shown in Fig. 4A. As the relationship between cells becomes more distant (from gold, to green to blue to red), the curve flattens, approaching that of randomly paired cells (Fig. 4A, grey).

We fit the mean difference of the time to enter apoptosis between cells from different generations to an exponential recovery curve (Fig. 4B). This revealed that the half-time of loss of apoptosis susceptibility was 1.3±0.6 generations, and as cells become more distantly related, the difference in their time of apoptosis should approach 86±9 minutes. The calculated time of apoptosis between distantly related cells (86±9 minutes) is within the error of the measured apoptosis time differences between unrelated cells (90±1 minutes), indicating that the similarity of the apoptotic state of related cells is transient, and does not result from genetic differences.

To examine the persistence of apoptosis susceptibility over more than four generations, we analyzed the distributions of the onset of DEVDase activation in clonal cell lines (supplementary material Fig. S8B). The overlap in the distributions was significant (One-way ANOVA: F=1.29, F_{crit}=2.38, $F<F_{crit}$), indicating that the similarity in apoptosis susceptibility does not persist indefinitely, and is unlikely to be due to genetic variation or the presence of multiple cell lineages.

Intragenerational divergence in apoptosis timing

We next plotted the difference in DEVDase activation as a function of the time since sister cells or cousin cells divided from their last common ancestor (Fig. 4C). An exponential recovery curve was fit to the data. To assess intragenerational trends, cell pairs were binned according to the time since division (500 minute bins; Fig. 4C). Apoptosis times between newly divided sister cells were more similar than between sister cells that had divided long before STS treatment (1 μM STS, Fig. 4C; 2 μM STS, supplementary material Fig. S8C,D). These results indicate that the loss of correlation of apoptosis between sister cells occurs continuously and not as a discrete step during mitosis, or another phase of the cell cycle.

Inhibition of divergence

To determine whether new protein expression was responsible for the divergence of apoptosis susceptibility, we inhibited protein expression in newly divided cells using CHX, which is an inhibitor of protein translation (Ennis and Lubin, 1964; Siegel and Sisler, 1963). In an asynchronous culture, we monitored newly divided HeLa cells under the following conditions: (1) in the presence of CHX (20 μg/ml) for 9 hours; (2) in the absence of CHX for 3 hours, followed by the presence of CHX for 6 hours; (3) in the absence of CHX for 6 hours, followed by the presence of CHX for 3 hours; and (4) in the absence of CHX for 9 hours. Cells were then treated with both CHX (20 μg/ml) and STS (1 μM) (supplementary material Fig. S9) to eliminate potential differences in apoptotis due to the presence or absence of CHX. The difference in apoptosis times was determined for sister cells, and compared for the different durations of CHX treatment. The longer the time that sister cells spent in the absence of CHX, the greater the difference in apoptosis times (Fig. 4D, supplementary material Fig. S9). The difference in sister cell apoptosis times for different CHX treatments was not a result of an overall difference in the time of apoptosis in the population (supplementary material Fig. S9). Similar results were observed with puromycin, which uses a different mechanism to inhibit protein synthesis (Traut and Monro, 1964) (supplementary material Fig. S10). These results suggest that the divergence of apoptosis times between sister cells is partially a result of new protein expression.

Discussion

Although sister cells undergo DEVDase activation at similar times relative to the population, this similarity could not be correlated with the position of cells in the cell cycle, nor with the distance between cells. By investigating the similarity of apoptosis susceptibility over subsequent generations, we observed a divergence in the times of apoptosis as cells become less related. A divergence in apoptosis susceptibility is also observed within single generations, and is limited by blocking protein synthesis after division. These results suggest that the signal transduction in response to apoptotic stimuli reflects the internal state of the cell and is therefore deterministic.

Entry into apoptosis is similar for cells in proximity

When studying the times of apoptosis in a population, we noticed that times for neighboring cells to enter apoptosis were highly correlated relative to more distant cells (Fig. 2). We first used three independent tests to demonstrate that there was no correlation between when DEVDases were activated and the physical distances between unrelated cells (Fig. 3). Thus, the secreted factors might either be acting only on the secreting cell itself or on the culture as a whole, but not affecting the local microenvironment.

Since recently divided cells both tend to be near each other and tend to be synchronized in the cell cycle, this might also account for the ‘local synchronization’. We therefore monitored apoptosis in cell-cycle-synchronized populations (supplementary material Fig. S5) or in an asynchronous population where the cell cycle phase was determined using a live cell reporter (supplementary material Fig. S6). However, in both assays there was no detectable correlation between cell cycle and apoptosis.

Entry into apoptosis is similar for related cells

When neighboring cells were categorized into sister cells, cousins or unrelated cells, sister cells showed the strongest correlation for the time of entering apoptosis (Fig. 4A). Apoptosis times of sister cells were most similar right after division, and this similarity decreased over time (Fig. 4C). When weaker apoptotic insults were used, we found that not only was the timing of apoptosis correlated for sister cells, but also the probably of undergoing apoptosis (Fig. 3E). Thus, fates are linked in sister cells.

Determinism in apoptosis signal transduction

The similarity of apoptosis times and the apoptotic fate of sister cells suggest that the time of apoptosis, and the fate of a single cell in response to an apoptosis stimulus is predictable. This predictability of apoptotic signal transduction suggests that cells that undergo apoptosis at a later time relative to the population might have molecular compositions that make the cell less susceptible to apoptosis, and do not result from stochastic events in apoptosis signal transduction. Although the difference in apoptosis time between sister cells is smaller than expected if the entry to apoptosis was stochastic, the apoptosis times of sister cells was not identical (Fig. 3C). Possible explanations for this include an asymmetrical dilution of factors during division, or that the molecular composition of daughter cells diverges after division. The latter explanation is consistent with results from Fig. 4C.

Divergence of apoptotic susceptibility

Sister and cousin cells underwent apoptosis at similar times, but as cells became more distantly related, the difference in their times of apoptosis increased (Fig. 4). This divergence of apoptotic susceptibility was observed to occur over a few generations, suggesting that the molecular composition of the cell that predisposes cells to apoptosis is transient. Our results are reminiscent of previous results on the variability of gene expression in a lineage of mammalian cells (Sigal et al., 2006). Sigal and co-workers calculated the kinetics and genealogical time over which the gene expression levels in a cell lineage reach the different expression levels found in the population. Strikingly, our half-time of divergence of the apoptosis response was on a similar scale as divergence in the gene expression study, thus suggesting that the divergence of gene expression levels in mammalian cells has a phenotypic consequence.

Divergence from new protein synthesis

The divergence of apoptosis times of sister cells was inhibited by blocking protein synthesis after division (Fig. 4D, supplementary material Figs S9 and S10), suggesting that variation in apoptosis is a result of a variation in protein synthesis just after division. Other molecular changes might contribute, including the degradation of proteins, the post-translational modifications of proteins, and the localization of proteins. We propose that if the molecular composition of the cell, and the underlying biochemical network used to process apoptotic triggers is similar between sister cells at the time of treatment, the apoptosis times will be similar. This composition could consist of both pro-apoptotic proteins and anti-apoptotic proteins, which might set a threshold (Albeck et al., 2008; Sheridan and Martin, 2008). However, as the molecular composition of cells start to drift apart, so does the apoptotic response. The divergence could be a fluctuation of a single protein, or more likely a group of proteins (Sigal et al., 2006). Furthermore, the cause of divergence for one pair of sister cells could have a different underlying cause for another pair. An understanding of this process and the type of threshold would be aided by monitoring gene expression in single cells (Cohen et al., 2008), or the ability to separate early and late apoptotic cells. Nonetheless, although the biochemical reactions triggered by an apoptotic signal might be deterministic, the same might not be true for reactions that determine the molecular composition of the cell before the addition of an apoptosis drug.

In summary, these results highlight the benefits of single-cell assays in addition to monitoring population phenotypes. In a population, there is a substantial distribution in the onset of apoptosis. This is not just a stochastic transduction of an apoptotic signal, but a difference resulting from population heterogeneity. The determinism of signal transduction in single cells should enable the observation of processes that are too rapid to be continuously imaged. This can be potentially done by waiting for a cell to undergo apoptosis at low imaging frequency, then imaging its sister cell or related cells, at a higher frequency. The symmetry of division reproduces the underlying biochemical networks that cells use to respond to external triggers. Exploitation of this symmetry by comparing responses in sister cells enables an understanding of the reproducibility of the response of these signaling networks, and provides insight in to how biochemical signals are transduced. It remains to be seen whether this similarity extends to other phenotypes, and whether it extends to phenotypes in vivo.

Materials and Methods

Cell culture

HeLa, NIH3T3, MEF and HT1080 cells were maintained at 5% CO_2 in DMEM containing 10% FBS. Apoptosis induced with staurosporine (Sigma), etoposide (BioVision, Mountain View, CA), TNFα (BioVision), cycloheximide (Sigma). Protein synthesis was inhibited using cycloheximide and puromycin (Sigma). Stable cell lines were generated using lentiviral infection and flow cytometry (BD FACS Aria, BD Biosciences, Flow Cytometry Facility at The Rockefeller University). Clonal stable cells were induced to undergo apoptosis 29 days after sorting single cells into single wells. Treatment regimes are shown in supplementary material Figs S9A and S10A. Medium with cycloheximide or puromycin was added through the top of the dish.

Plasmid constructs and cell culture

Primers used to construct reporters are described in supplementary material Table S2. pmDEVD was created by inserting a palmitoylation sequence from pECFPmem (Clontech) along with the DEVD sequence into the pECFP-C1 vector (Clontech). pmControl was created using a similar strategy without the DEVD sequence. The pCaspase-3 sensor was modified to enable use of different fluorescent proteins. erDEVD was created by inserting residues 1-68 from Sec63 into the modified pCaspase-3 reporter. FRET-DEVD was created by PCR amplification of CyPet and yPet along with the DEVD site into the pEGFP-C1 vector (Clontech). We used the fluorophores mCerulean, mCitrine and mCherry for the non-FRET constructs. CyPet and yPet (optimized from CFP and YFP respectively) were used in the FRET construct. mCherry and mCitrine were obtained from Roger Tsien (Shaner et al., 2004). CyPet and yPet obtained from Patrick Daugherty (Nguyen and Daugherty, 2005). mCerulean was obtained from David Piston (Rizzo et al., 2004). PSLD-mCitrine was created by inserting the PSLD domain (residues 957-1087 of human DNA Helicase B). Cerulean-NLS was created by inserting the nuclear localization tag from pEYFP-Nuc (Clontech) at the C-terminus of mCerulean. Cells were transiently transfected with Lipofectamine 2000 (Invitrogen).

Fluorescence microscopy

Confocal imaging was performed on a Zeiss510 confocal microscope using a ×60 objective (BioImaging Facility, The Rockefeller University). Cells were maintained at 37°C using a Warner Heating Chamber, and were imaged in Cell Imaging Media [Hanks BBS (Sigma) 9.8 g/l, 10 mM HEPES, 5% FBS, pH 7.4]. The following fluorophores were imaged with the following filters: mCerulean, 458 excitation, 458/514 dichroic, NFT515 Mirror, 473-498 emission filters; mCitrine, 514 excitation, 458/514 dichroic, NFT515 Mirror, 550/50 emission filters; mCherry, 543 excitation, 405/514/543 dichroic, NFT545 Mirror, 560 LP emission filters.

Wide-field imaging performed on an Olympus IX81 microscope with ×10 or ×60 objectives, automated stage (Prior Scientific) and Metamorph (Molecular Devices, Sunnyvale, CA) data acquisition software. Fluorophores and their imaging conditions were as follows: mCerulean, ET 430/24 excitation filter, ET470/24 emission filter; mCitrine: ET 500/20 excitation filter, ET 535/30 emission filter; mCherry, ET 577/25 excitation filter, ET 632/60 emission filter; DAPI, 360/40 excitation filter, 400/LP emission filter. Long-term imaging was performed in 24-well dishes to increase the number of cell conditions per experiment. At least three fields per well were acquired. Medium exchange occurred via tubes inserted through the top of the dishes. Long-term imaging occurred for between 24 hours and 92 hours. Untreated cells appeared normal at 92 hours.

Reporter characterization

Imaging data was initially analyzed with Metamorph. To quantify changes in the pmDEVD reporter, a single region within the cytoplasm was chosen. Fluorescent proteins fused to the palmitoylation domain localize to the Golgi as well as the plasma membrane. Therefore in choosing a cytoplasmic region to quantify the changes in fluorescence, the Golgi aggregate fluorescence was avoided. To quantify fluorescent changes in the erDEVD reporter and the pCaspase-3 sensor, we monitored nuclear fluorescence. The FRET ratio was calculated as CFP/YFP after background subtraction. TUNEL staining of STS (2 μM) treated HeLa cells performed in glass-bottom 96-well plates (BDBiosciences). In each well, we determined whether cells were TUNEL positive, and transfected with the pmDEVD-mCherry reporter. The percentage of TUNEL-positive cells for transfected and untransfected cells was calculated, and averaged over three wells for each time point (supplementary material Fig. S4H).

Cell cycle analysis

Cell tracking and analysis of the G1-S transition was performed in Imaris (using the Spot Module) (Bitplane, St Paul, MN). The nucleus was tracked using Cerulean-NLS. The time of the G1-S transition was characterized as the time when the mCitrine-PSLD nuclear fluorescence irreversibly decreased from the basal G1 levels (see supplementary material Fig. S6 for an example of the PSLD-mCitrine time-course data). Alternatively, cell cycles were synchronized with a double thymidine block (15 hour block, 10 hour release, 15 hour block) and released for variable times (supplementary material Fig. S5). Controls to determine DNA content were performed with Hoechst 33342 (Sigma) staining (supplementary material Fig. S5). Briefly, cells were trypsinized, fixed in 4% paraformaldehyde, stained with Hoechst 33342 (1 μg/ml, 20 minutes), and analyzed with BD LSRII flow cytometry analyzer (BD BioScience). One-way ANOVA was performed in Excel.

Correlation between inter-cell distance and DEVDase activation

The determination of the position of cells and their times of apoptosis was performed in Metamorph and Excel. The position of cells was the position at the time of drug treatment. Analysis of the distance between cells and their times of apoptosis was performed in MatLab using the position of cells and time of DEVDase activation. Distance was calculated as the distance between the approximate center of cells, and not the edges of cells. This data was binned based on distance, producing plots in Fig. 2B and Fig. 3A,B. Error bars indicate the 95% confidence interval of the mean.

For analysis of inter-cell distance and DEVDase activation for cells that were not sister or cousin cells, we performed the same analysis as above, but excluded sister or cousin comparisons from the calculation. Analysis of plating at different times and correlating distance to difference in DEVDase activation was performed as above. The times of the actual DEVDase activation difference was normalized to the DEVDase activation difference for cells whose position were randomly reassigned (null hypothesis). This was a result of variability in the apoptosis time difference for cells that are very far apart at the different plating times.

Analysis of sister cells and cell lineage

Sister cell pairs were visually determined by monitoring division up to 36 hours before drug treatment. Comparisons of the average time of apoptosis for different cell types and different stimuli (Fig. 3D) was calculated in Excel. The randomized differences were calculated by taking actual times of apoptosis and randomly pairing these in Excel. Cell death of only part of the population (44% of the population) was induced by using a 1 μM STS treatment for 45 minutes. Cells were washed three times in fresh DMEM after treatment. Within 36 hours of drug treatment, there were some cells that did not divide or undergo apoptosis. We counted these non-apoptotic, non-dividing cells as surviving. Chi-squared tests were performed with P calculated for two degrees of freedom (Fig. 3E).

Analysis of the difference in apoptosis between related cells was performed in MatLab (Fig. 4A). Histograms were plotted in Excel. Data fit for the memory of the cell was performed using the Marquadt-Levenberg Algorithm in Origin or non-linear least squares fit algorithm in MatLab using all the data points, and not the average data points. One-way ANOVA of apoptosis times of clonal cell lines was performed in Excel with F_{crit} determined by Excel for α=0.05 (supplementary material Fig. S8). A subset of sister cells from Fig. 4A was re-analyzed to determine both the time of apoptosis, and the time since division. Cells were fit to recovering exponential curve as performed in MatLab with calculations for the 95% confidence interval of the fit (Fig. 4C). Cells were grouped into bins of 500 minutes to demonstrate intra-generational trends using Excel (Fig. 4C). Error bars for this binned data represent 95% confidence interval of the mean.

We thank Roger Tsien, David Piston and Patrick Daugherty for plasmids, Simon lab members for advice and technical support, and Shai Shaham and Hermann Steller for discussions. We thank The Rockefeller University Bioimaging Facility, The Rockefeller University Flow Cytometry Facility, and the ADARC Flow Cytometry facility for discussion and technical support. We are grateful for the support of NSF BES-0620813 and NIH P20 GM072015 (to S.M.S.). Deposited in PMC for release after 12 months.

References

Abkowitz, J. L., Catlin, S. N. and Guttorp, P. (1996). Evidence that hematopoiesis may be a stochastic process in vivo. *Nat. Med.* **2**, 190-197.

Albeck, J. G., Burke, J. M., Aldridge, B. B., Zhang, M., Lauffenburger, D. A. and Sorger, P. K. (2008). Quantitative analysis of pathways controlling extrinsic apoptosis in single cells. *Mol. Cell* **30**, 11-25.

Arkin, A., Ross, J. and McAdams, H. H. (1998). Stochastic kinetic analysis of developmental pathway bifurcation in phage lambda-infected Escherichia coli cells. *Genetics* **149**, 1633-1648.

Cohen, A. A., Geva-Zatorsky, N., Eden, E., Frenkel-Morgenstern, M., Issaeva, I., Sigal, A., Milo, R., Cohen-Saidon, C., Liron, Y., Kam, Z. et al. (2008). Dynamic proteomics of individual cancer cells in response to a drug. *Science* **322**, 1511-1516.

Danial, N. N. and Korsmeyer, S. J. (2004). Cell death: critical control points. *Cell* **116**, 205-219.

Ellis, R. E., Yuan, J. Y. and Horvitz, H. R. (1991). Mechanisms and functions of cell death. *Annu. Rev. Cell Biol.* **7**, 663-698.

Ennis, H. L. and Lubin, M. (1964). Cycloheximide: Aspects of inhibition of protein synthesis in mammalian cells. *Science* **146**, 1474-1476.

Enver, T., Heyworth, C. M. and Dexter, T. M. (1998). Do stem cells play dice? *Blood* **92**, 348-351.

Goldstein, J. C., Waterhouse, N. J., Juin, P., Evan, G. I. and Green, D. R. (2000). The coordinate release of cytochrome c during apoptosis is rapid, complete and kinetically invariant. *Nat. Cell Biol.* **2**, 156-162.

Liu, X., Zou, H., Slaughter, C. and Wang, X. (1997). DFF, a heterodimeric protein that functions downstream of caspase-3 to trigger DNA fragmentation during apoptosis. *Cell* **89**, 175-184.

Nguyen, A. W. and Daugherty, P. S. (2005). Evolutionary optimization of fluorescent proteins for intracellular FRET. *Nat. Biotechnol.* **23**, 355-360.

Ow, Y. L., Green, D. R., Hao, Z. and Mak, T. W. (2008). Cytochrome c: functions beyond respiration. *Nat. Rev. Mol. Cell. Biol.* **9**, 532-542.

Rehm, M., Dussmann, H. and Prehn, J. H. (2003). Real-time single cell analysis of Smac/DIABLO release during apoptosis. *J. Cell Biol.* **162**, 1031-1043.

Rizzo, M. A., Springer, G. H., Granada, B. and Piston, D. W. (2004). An improved cyan fluorescent protein variant useful for FRET. *Nat. Biotechnol.* **22**, 445-449.

Salvesen, G. S. and Dixit, V. M. (1997). Caspases: intracellular signaling by proteolysis. *Cell* **91**, 443-446.

Schotte, P., Declercq, W., Van Huffel, S., Vandenabeele, P. and Beyaert, R. (1999). Non-specific effects of methyl ketone peptide inhibitors of caspases. *FEBS Lett.* **442**, 117-121.

Shaner, N. C., Campbell, R. E., Steinbach, P. A., Giepmans, B. N., Palmer, A. E. and Tsien, R. Y. (2004). Improved monomeric red, orange and yellow fluorescent proteins derived from Discosoma sp. red fluorescent protein. *Nat. Biotechnol.* **22**, 1567-1572.

Sheridan, C. and Martin, S. J. (2008). Commitment in apoptosis: slightly dead but mostly alive. *Trends Cell Biol.* **18**, 353-357.

Siegel, M. R. and Sisler, H. D. (1963). Inhibition of protein synthesis in vitro by cycloheximide. *Nature (London)* **200**, 675-676.

Sigal, A., Milo, R., Cohen, A., Geva-Zatorsky, N., Klein, Y., Liron, Y., Rosenfeld, N., Danon, T., Perzov, N. and Alon, U. (2006). Variability and memory of protein levels in human cells. *Nature (London)* **444**, 643-646.

Skene, J. H. and Virag, I. (1989). Posttranslational membrane attachment and dynamic fatty acylation of a neuronal growth cone protein, GAP-43. *J. Cell Biol.* **108**, 613-624.

Spudich, J. L. and Koshland, D. E., Jr (1976). Non-genetic individuality: chance in the single cell. *Nature (London)* **262**, 467-471.

Thornberry, N. A., Rano, T. A., Peterson, E. P., Rasper, D. M., Timkey, T., Garcia-Calvo, M., Houtzager, V. M., Nordstrom, P. A., Roy, S., Vaillancourt, J. P. et al. (1997). A combinatorial approach defines specificities of members of the caspase family and granzyme B. Functional relationships established for key mediators of apoptosis. *J Biol. Chem.* **272**, 17907-17911.

Traut, R. R. and Monro, R. E. (1964). The puromycin reaction and its relation to protein synthesis. *J. Mol. Biol.* **10**, 63-72.

Weinberger, L. S., Burnett, J. C., Toettcher, J. E., Arkin, A. P. and Schaffer, D. V. (2005). Stochastic gene expression in a lentiviral positive-feedback loop: HIV-1 Tat fluctuations drive phenotypic diversity. *Cell* **122**, 169-182.

Wyllie, A. H. (1980). Glucocorticoid-induced thymocyte apoptosis is associated with endogenous endonuclease activation. *Nature (London)* **284**, 555-556.

Xu, F., Carlos, T., Li, M., Sanchez-Sweatman, O., Khokha, R. and Gorelik, E. (1998). Inhibition of VLA-4 and up-regulation of TIMP-1 expression in B16BL6 melanoma cells transfected with MHC class I genes. *Clin. Exp. Metastasis* **16**, 358-370.

Yuan, J., Shaham, S., Ledoux, S., Ellis, H. M. and Horvitz, H. R. (1993). The C. elegans cell death gene ced-3 encodes a protein similar to mammalian interleukin-1 beta-converting enzyme. *Cell* **75**, 641-652.

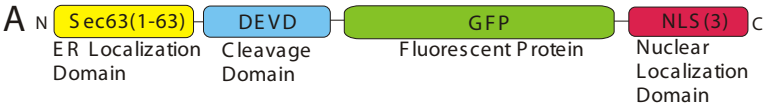
A
N
Sec63(1-63)
DEVD
GFP
NLS(3)
C
ER Localization Domain
Cleavage Domain
Fluorescent Protein
Nuclear Localization Domain


B

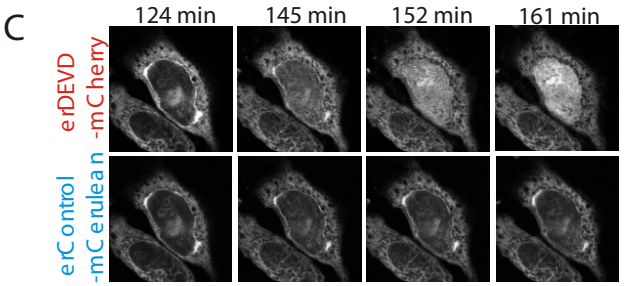
C
124 min
145 min
152 min
161 min
erDEVD-mCherry
erControl-mCerulean

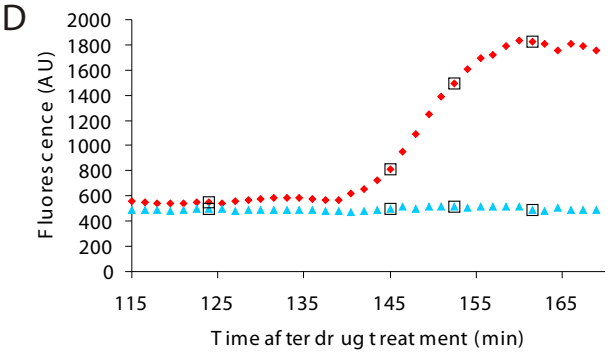
D
Fluorescence (AU)
2000
1800
1600
1400
1200
1000
800
600
400
200
0
115
125
135
145
155
165
Time after drug treatment (min)

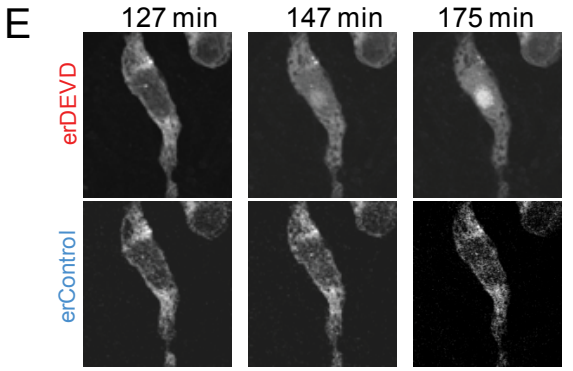
E
127 min
147 min
175 min
erDEVD
erControl

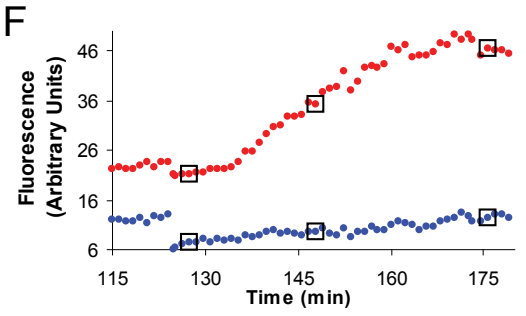
F
Fluorescence (Arbitrary Units)
46
36
26
16
6
115
130
145
160
175
Time (min)

A

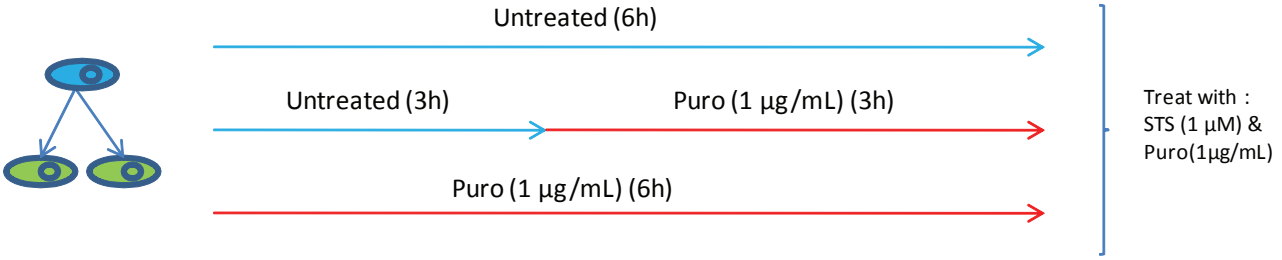
Untreated (6h)
Untreated (3h)
Puro (1 µg/mL) (3h)
Puro (1 µg/mL) (6h)
Treat with :
STS (1 µM) &
Puro(1µg/mL)

B

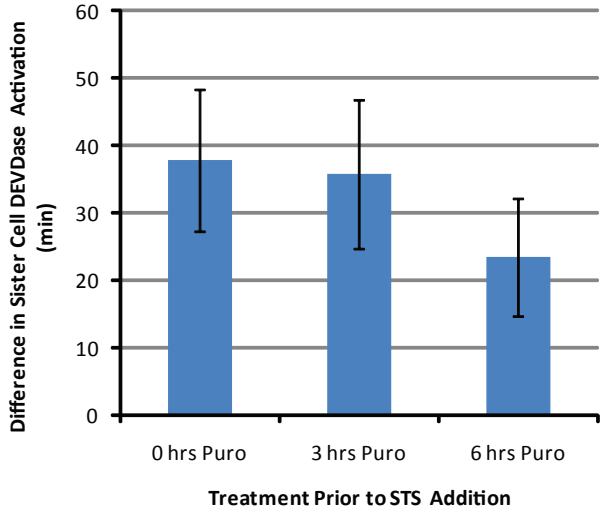
Difference in Sister Cell DEVDase Activation (min)
60
50
40
30
20
10
0
0 hrs Puro
3 hrs Puro
6 hrs Puro
Treatment Prior to STS Addition

C

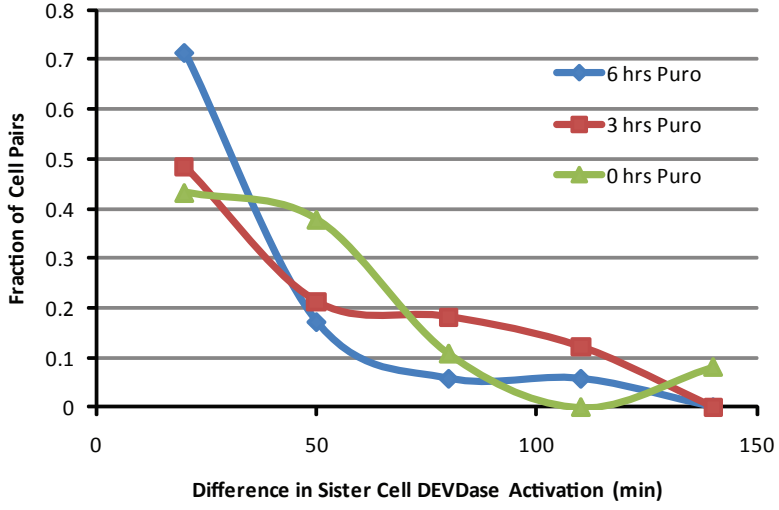
Fraction of Cell Pairs
0.8
0.7
0.6
0.5
0.4
0.3
0.2
0.1
0
6 hrs Puro
3 hrs Puro
0 hrs Puro
0
50
100
150
Difference in Sister Cell DEVDase Activation (min)

D

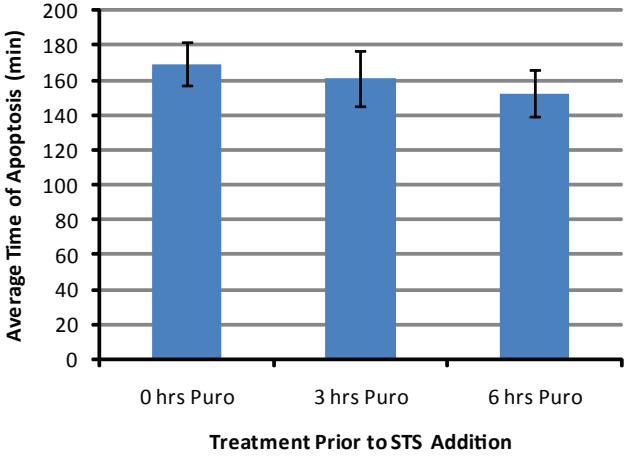
Average Time of Apoptosis (min)
200
180
160
140
120
100
80
60
40
20
0
0 hrs Puro
3 hrs Puro
6 hrs Puro
Treatment Prior to STS Addition

E

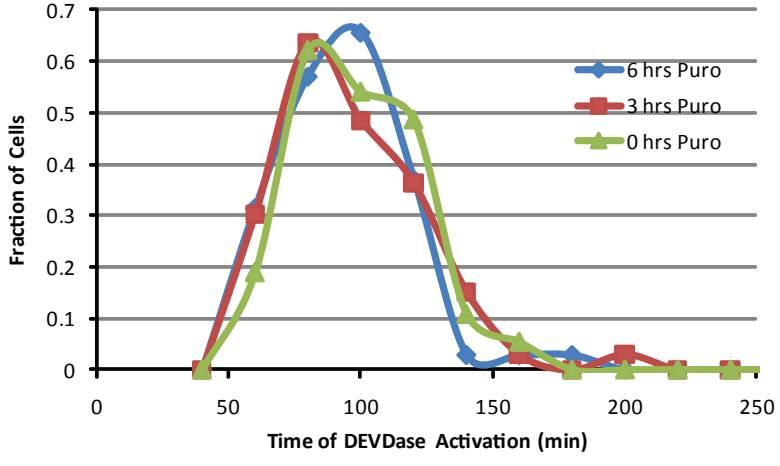
Fraction of Cells
0.7
0.6
0.5
0.4
0.3
0.2
0.1
0
6 hrs Puro
3 hrs Puro
0 hrs Puro
0
50
100
150
200
250
Time of DEVDase Activation (min)

Table S1

pmDEVD	Palmitoylation- sselsg**devd**gssgsefssstg-Fluorophore
pmControl	Palmitoylation-sselsgggssgstg-Fluorophore
erDEVD	Sec63(1-68)-sselsg**devd**gssgstg-Fluorophore-NLS(3)
erControl	Sec63(1-68)- sselsggssgstg -Fluorophore-NLS(3)
FRET-DEVD	CyPet–sselsg**devd**gssgsef-yPet

Table S2

Mem forward primer	GCGCGCTAGCAATAGATCTTGTTTAGTGAACATGCTGTGC TGTATGAGA
Me reverse primer	GATGAGGACCAAAAGATCTCATCGTCTGAATTGTCTGGTG ATGAAGTTGATGGAT CTTCTGGTTCTGAATTCGCGC
Fp forward primer	GCGCGAATTCTCATCTACCGGTATGGTGAGCAAGGGCGA G
Fp reverse primer	ATGGACGAGCTGTACAAGCTCGAGCATAACTAAGGATCC GCGC
Pm Control forward primer	GCGCGCTAGCAATAGATCTTGTTTAGTGAACATGCTGTGC TGTATGAGA
Pm control reverse primer	GATGAGGACCAAAAGATCTCATCGTCTGAATTGTCTGGTG GATCTTCTGGTTCTGAATTCGCGC
Nes forward primers	GCGCGCTAGCAATAGATCTTGTTTAGTGAACATGAACCTG GTGGACCTC
Nes reverse primer	GAGCTGGACGAGCAGCAGGAATTCTCATCGTCTGAATTG TCTGGTGATGAAGTTGATGGATCTTCTGGTTCTTCATCTA CCGGTGCGC
Fp forward primer	GCGCACCGGTATGGTGAGCAAGGGCGAG
Fp reverse primer	ATGGACGAGCTGTACAAGCTCGAGCATAACTAAGGATCC GCGC
Nls forward primer	GCGCCTCGAGTCTGATCCAAAAAAGAAGAGA
Nls reverse primer	GGATCCACCGGATCTAGATAAGGATCCGCGC
Nes control primer	GCGCGAATTCTCATCGTCTGAATTGTCTGGTGGATCTTCT GGTTCT
Nes control primer	ATGGACGAGCTGTACAAGCTCGAGCATAACTAAGGATCC GCGC
erDEVD forward primer	GCGCGCTAGCATGGCCGGGCAGCAGTTC
Er DEVD reverse primer	TGGTATCGTAAGCTTTCTGAATTCGCGC
FRET 1F	GCGCGCTAGCATGGTGAGCAAGGGAGAG
FRET 1R	ATGGACGAACTGTACAAATCCTCGTCCGAGCTCAGCGGA GATGAGGTCGATGGATCCCCAAA
FRET 2F	TTTGGGGATCCAGCGGAAGCGAATTCTCTTCAACCGGTAT GGTGAGCAAAGGCGAAGAG
FRET 2R	AACGAGCTCTATAAGTAAAAGCTTGCGC
PSLD F	GCGCCTCGAGCTTCTAGCGGCGCACCTCCA
PSLD R	GATAATCAAGAAACTTAGGAATTCGCGC

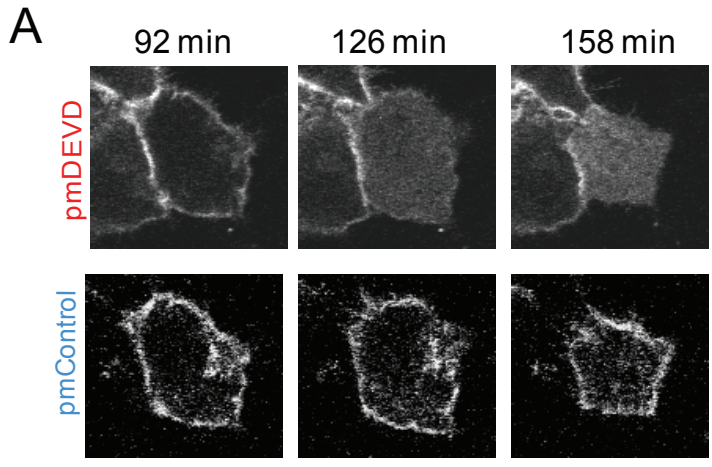
A
92 min
126 min
158 min
pmDEVD
pmControl

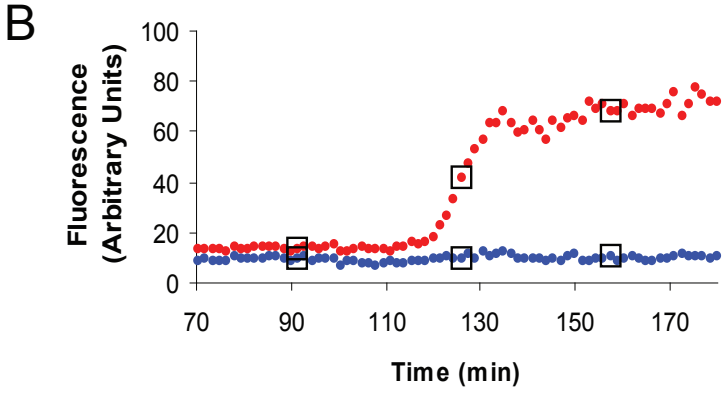
B
Fluorescence (Arbitrary Units)
100
80
60
40
20
0
70
90
110
130
150
170
Time (min)

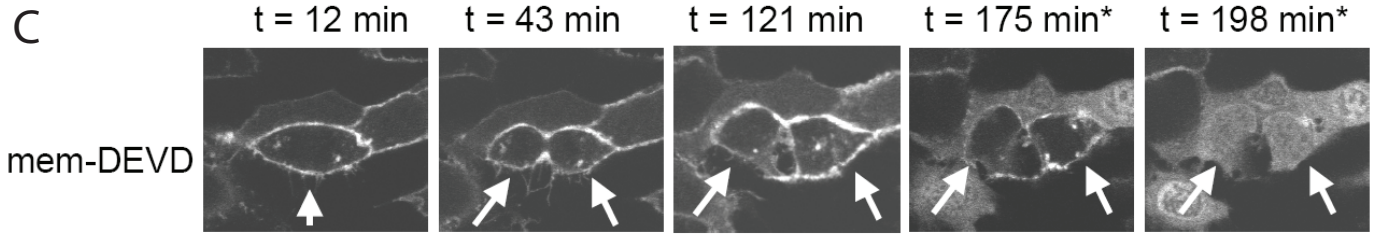
C
t = 12 min
t = 43 min
t = 121 min
t = 175 min*
t = 198 min*
mem-DEVD

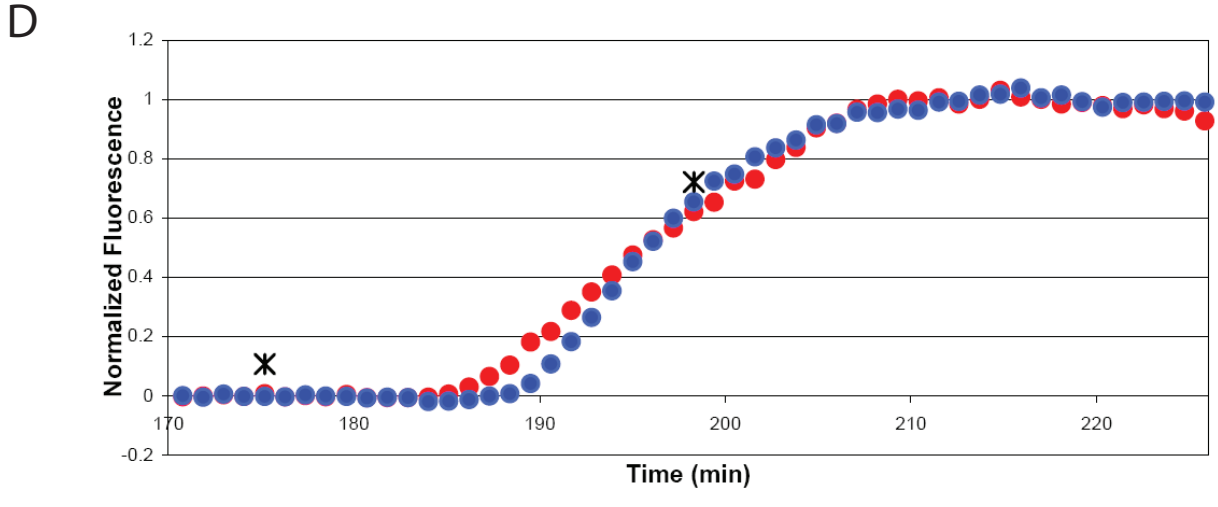
D
Normalized Fluorescence
1.2
1
0.8
0.6
0.4
0.2
0
-0.2
170
180
190
200
210
220
Time (min)

. A pmDEVD-mCherry

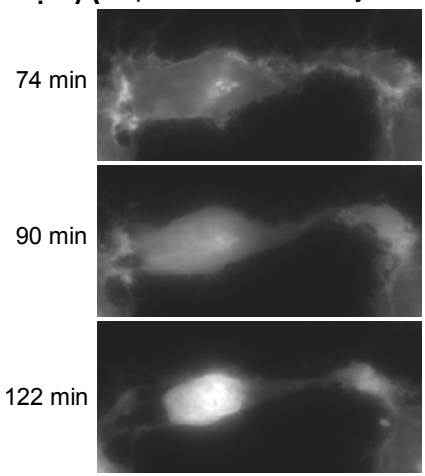

. B

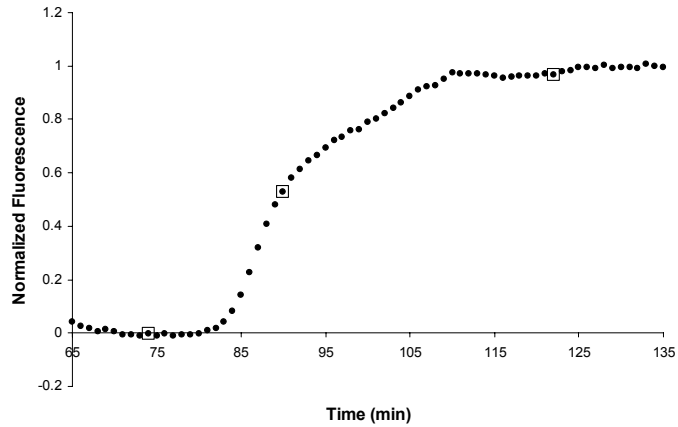

C

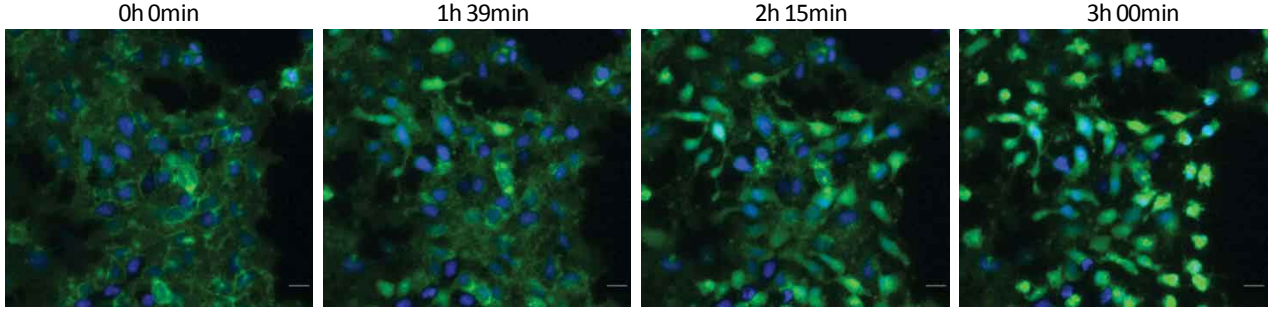

D

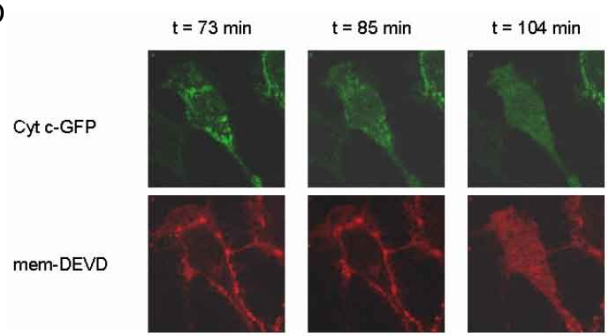

E

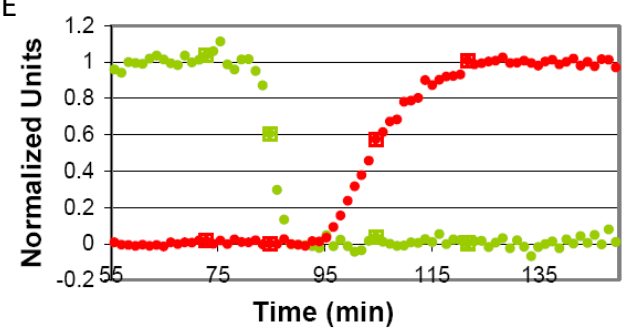

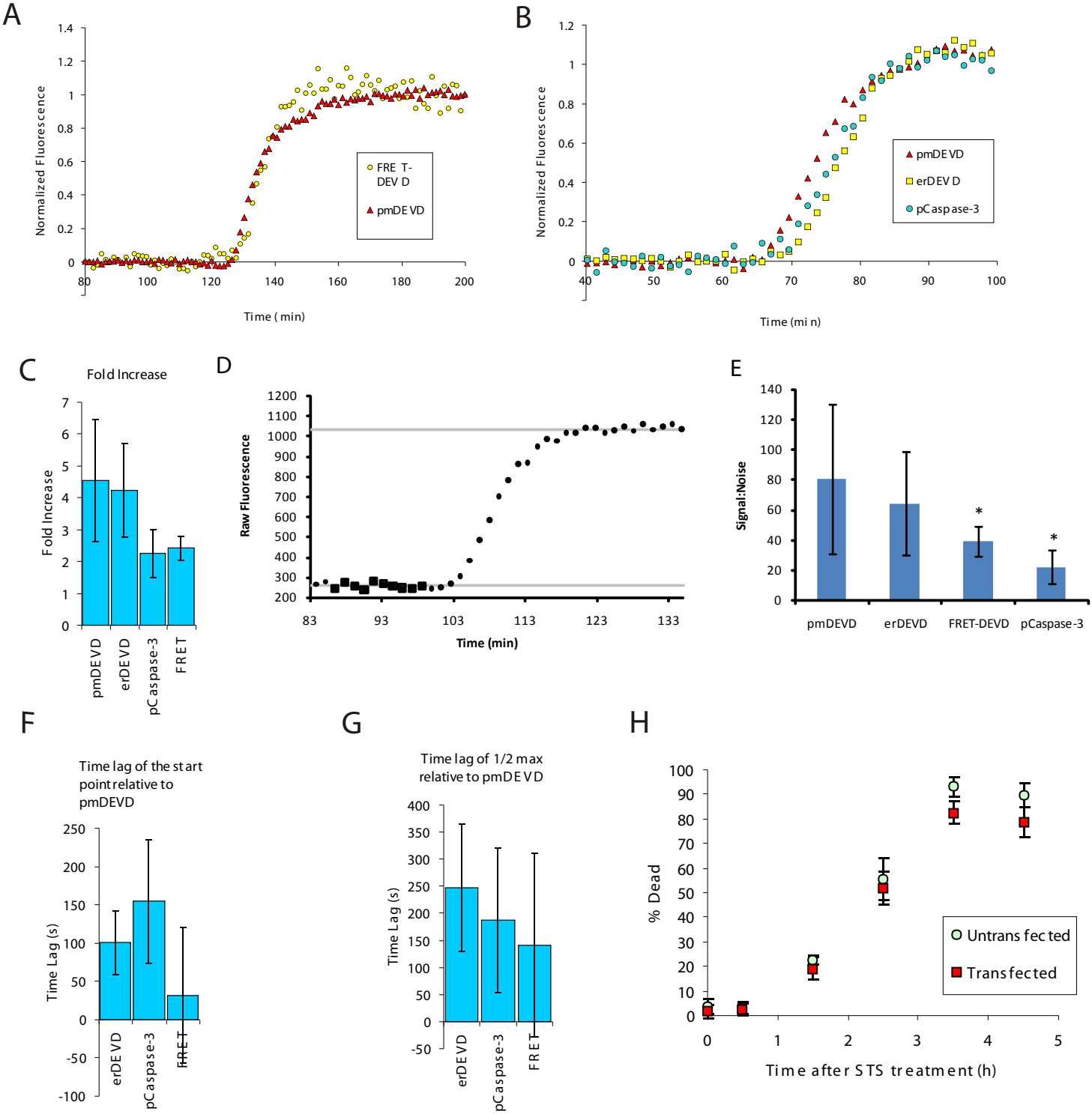
A
Normalized Fluorescence
Time (min)
FRET-DEVD
pmDEVD
B
Normalized Fluorescence
Time (min)
pmDEVD
erDEVD
pCaspase-3
C
Fold Increase
Fold Increase
pmDEVD
erDEVD
pCaspase-3
FRET
D
Raw Fluorescence
Time (min)
E
Signal:Noise
pmDEVD
erDEVD
FRET-DEVD
pCaspase-3
F
Time lag of the start point relative to pmDEVD
Time Lag (s)
erDEVD
pCaspase-3
FRET
G
Time lag of 1/2 max relative to pmDEVD
Time Lag (s)
erDEVD
pCaspase-3
FRET
H
% Dead
Untransfected
Transfected
Time after STS treatment (h)

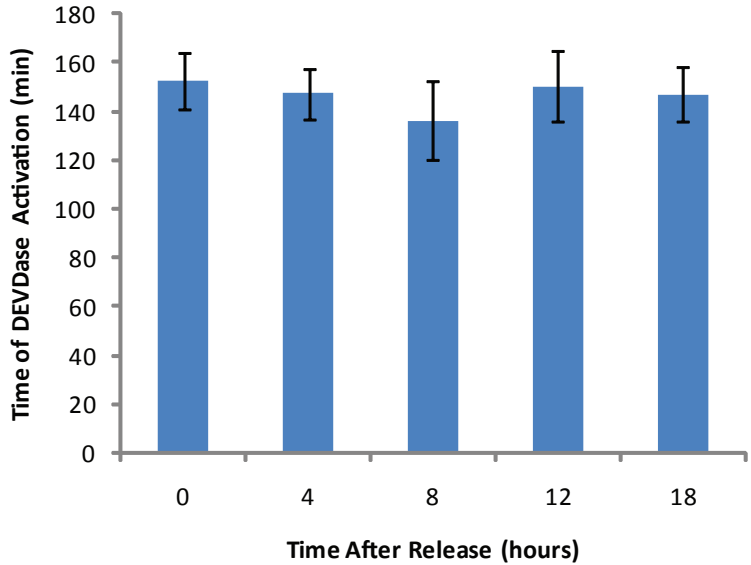
Time of DEVDase Activation (min)
180
160
140
120
100
80
60
40
20
0
0
4
8
12
18
Time After Release (hours)

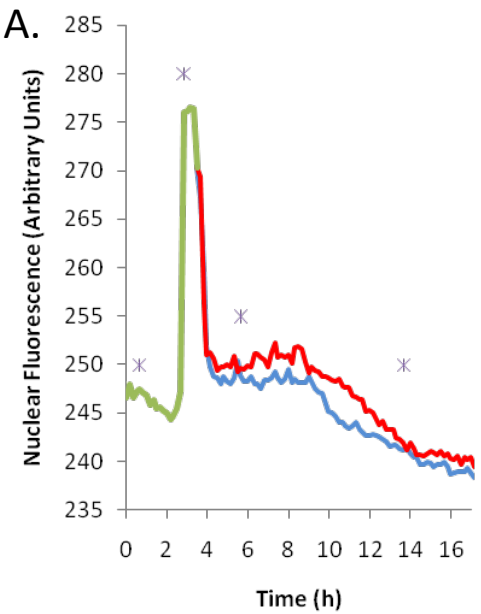
A.
Nuclear Fluorescence (Arbitrary Units)
285
280
275
270
265
260
255
250
245
240
235
0 2 4 6 8 10 12 14 16
Time (h)

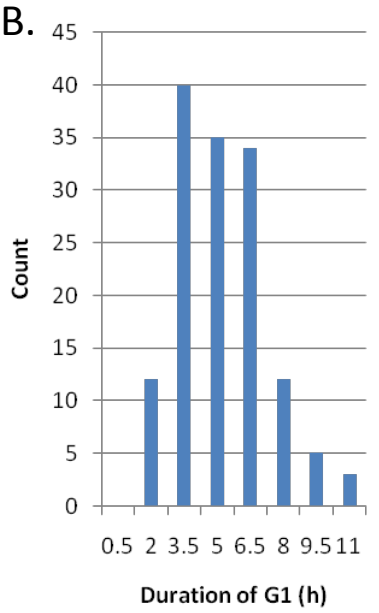
B.
Count
45
40
35
30
25
20
15
10
5
0
0.5 2 3.5 5 6.5 8 9.5 11
Duration of G1 (h)

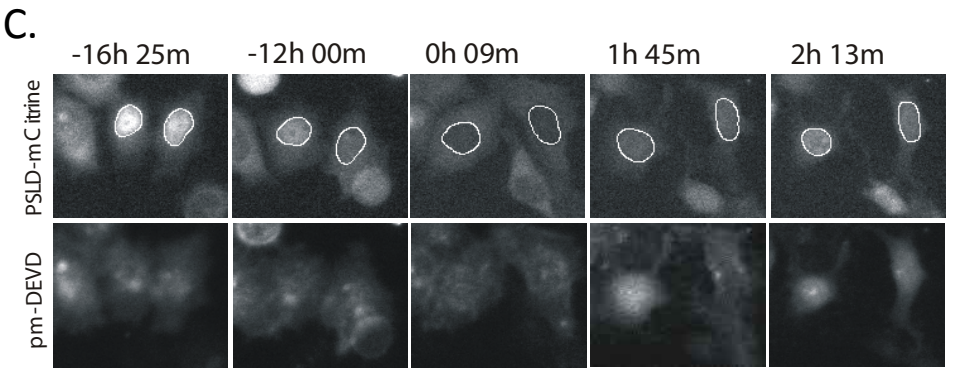
C.
-16h 25m
-12h 00m
0h 09m
1h 45m
2h 13m
PSLD-mCitrine
pm-DEVD

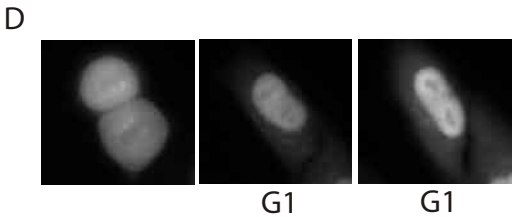
D
G1
G1

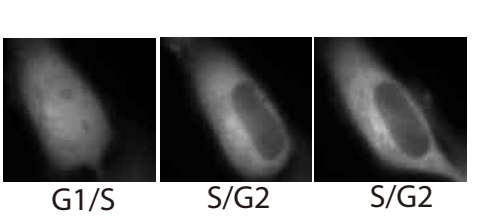
E
G1/S
S/G2
S/G2

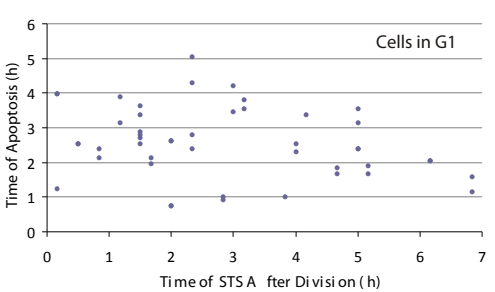
F
Cells in G1
Time of Apoptosis (h)
6
5
4
3
2
1
0
0 1 2 3 4 5 6 7
Time of STS After Division (h)

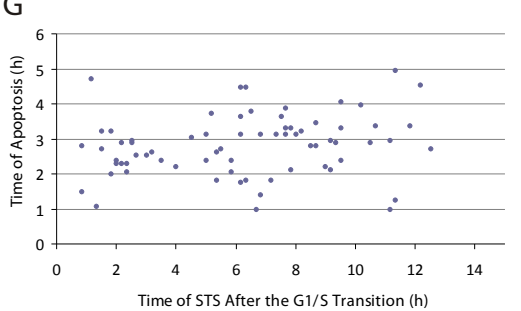
G
Time of Apoptosis (h)
6
5
4
3
2
1
0
0 2 4 6 8 10 12 14
Time of STS After the G1/S Transition (h)

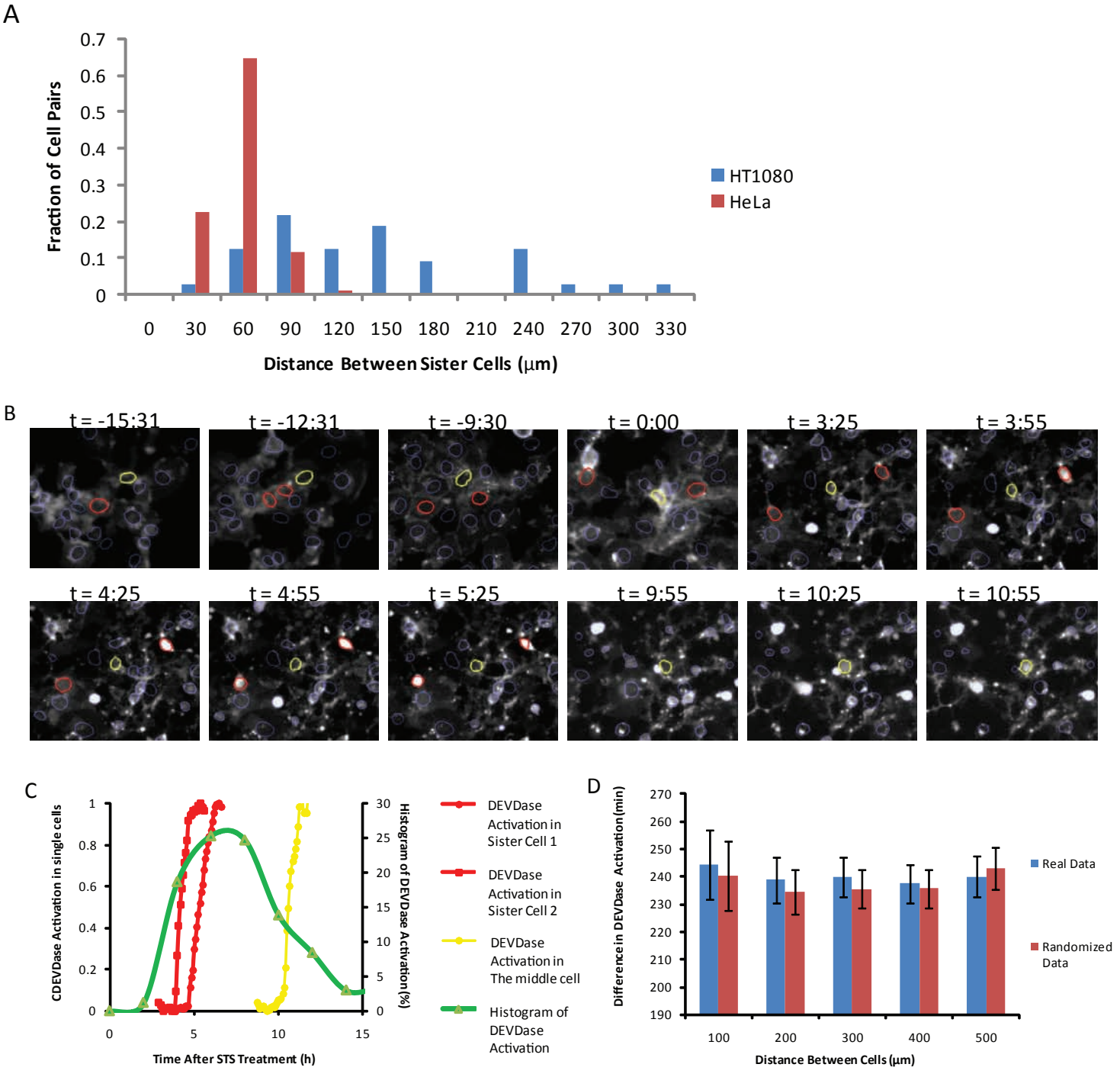
A
Fraction of Cell Pairs
0.7
0.6
0.5
0.4
0.3
0.2
0.1
0
0 30 60 90 120 150 180 210 240 270 300 330
Distance Between Sister Cells (μm)
HT1080
HeLa
B
t = -15:31
t = -12:31
t = -9:30
t = 0:00
t = 3:25
t = 3:55
t = 4:25
t = 4:55
t = 5:25
t = 9:55
t = 10:25
t = 10:55
C
CDEVDase Activation in single cells
Histogram of DEVDase Activation (%)
Time After STS Treatment (h)
DEVDase Activation in Sister Cell 1
DEVDase Activation in Sister Cell 2
DEVDase Activation in The middle cell
Histogram of DEVDase Activation
D
Difference in DEVDase Activation (min)
Distance Between Cells (μm)
Real Data
Randomized Data

A

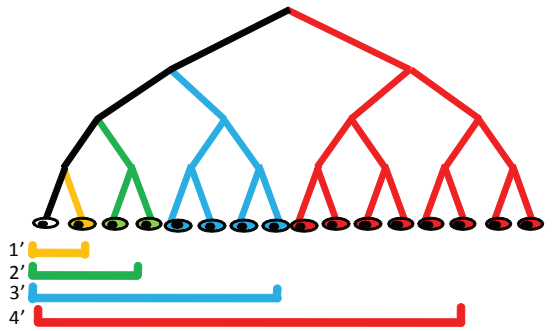
1'
2'
3'
4'

B

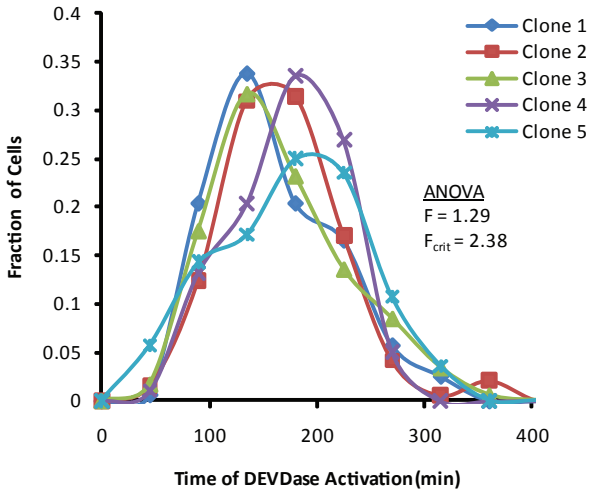
Clone 1
Clone 2
Clone 3
Clone 4
Clone 5
ANOVA
F = 1.29
F_crit = 2.38
Fraction of Cells
Time of DEVDase Activation (min)

C

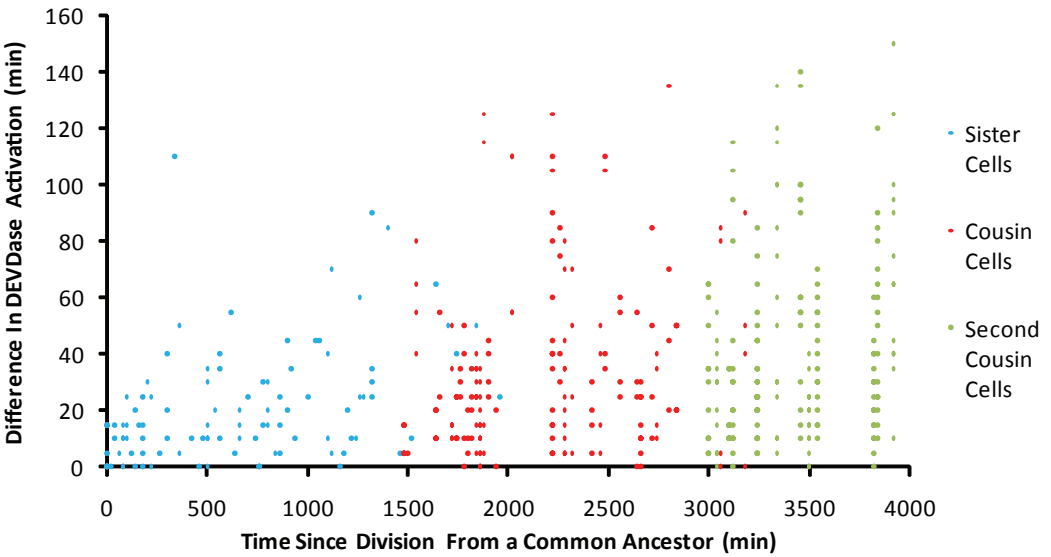
Difference In DEVDase Activation (min)
Time Since Division From a Common Ancestor (min)
Sister Cells
Cousin Cells
Second Cousin Cells

D

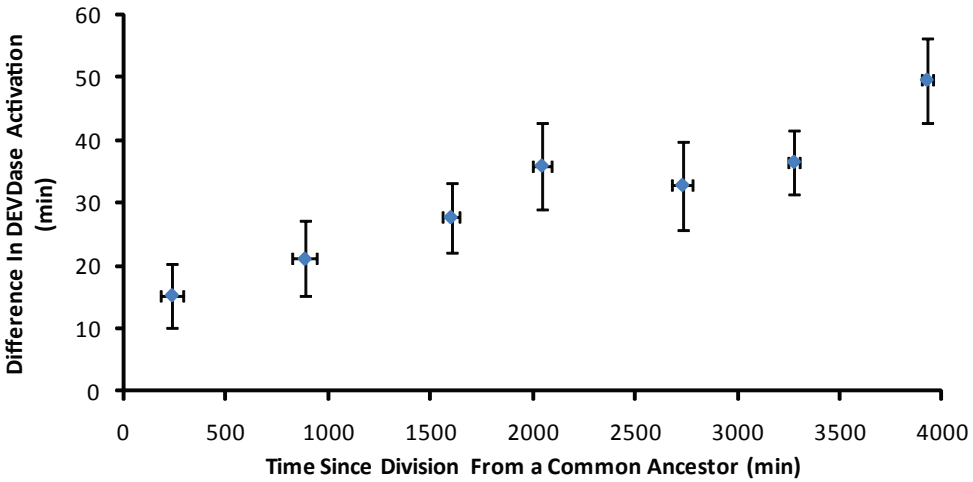
Difference In DEVDase Activation (min)
Time Since Division From a Common Ancestor (min)

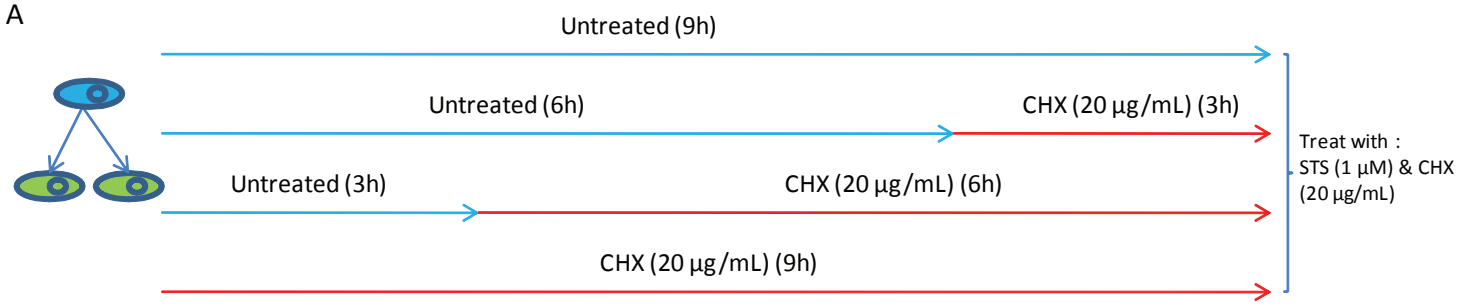
A
Untreated (9h)
Untreated (6h)
CHX (20 µg/mL) (3h)
Untreated (3h)
CHX (20 µg/mL) (6h)
CHX (20 µg/mL) (9h)
Treat with :
STS (1 µM) & CHX
(20 µg/mL)

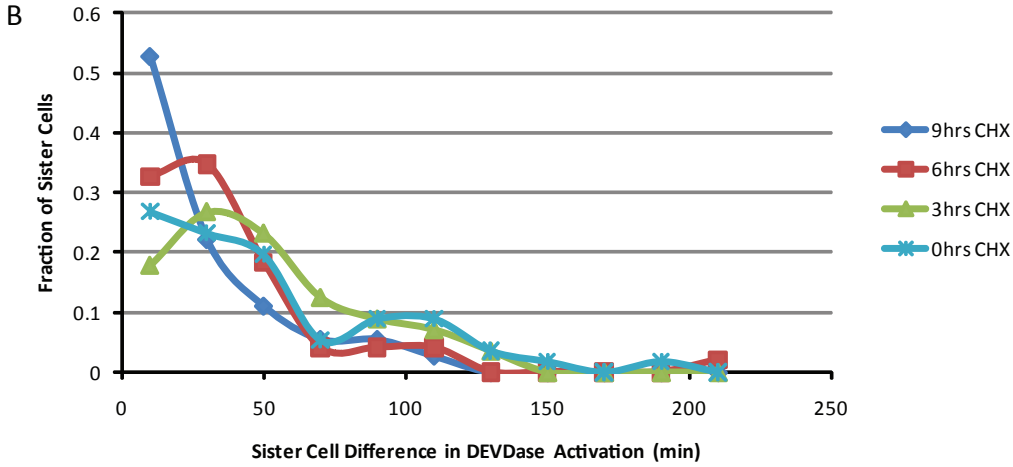
B
Fraction of Sister Cells
0.6
0.5
0.4
0.3
0.2
0.1
0
0
50
100
150
200
250
Sister Cell Difference in DEVDase Activation (min)
9hrs CHX
6hrs CHX
3hrs CHX
0hrs CHX

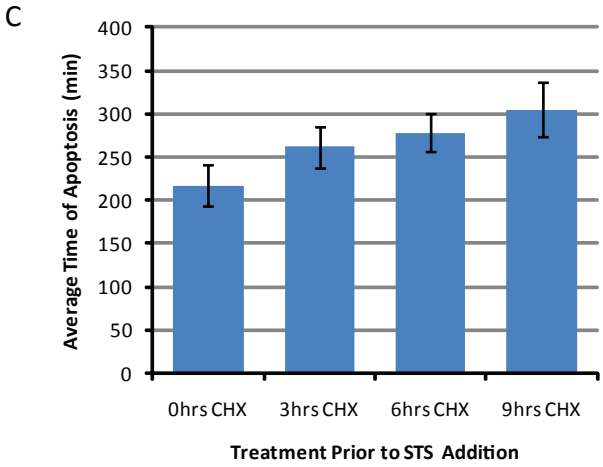
C
Average Time of Apoptosis (min)
400
350
300
250
200
150
100
50
0
0hrs CHX
3hrs CHX
6hrs CHX
9hrs CHX
Treatment Prior to STS Addition

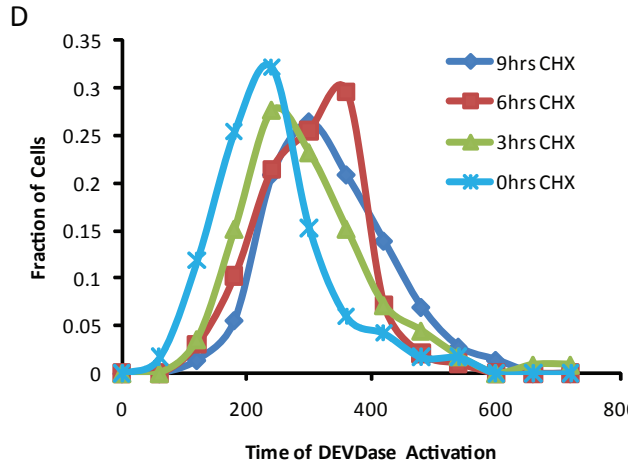
D
Fraction of Cells
0.35
0.3
0.25
0.2
0.15
0.1
0.05
0
0
200
400
600
800
Time of DEVDase Activation
9hrs CHX
6hrs CHX
3hrs CHX
0hrs CHX